British Journal of Nutrition (2019), 122, 1062–1072
doi:10.1017/S0007114519001740

Proteomics study of the effect of high-fat diet on rat liver

Jian Sang[1,2]†, Hengxian Qu[1,2]†, Ruixia Gu[1,2], Dawei Chen[1,2], Xia Chen[1,2], Boxing Yin[1,2], Yingping Huang[3], Wenbo Xi[3], Chunlei Wang[3] and Yujun Huang[1,2]*

[1]*College of Food Science and Technology, Yangzhou University, Yangzhou, Jiangsu 225127, People's Republic of China*
[2]*Key Lab of Dairy Biotechnology and Safety Control, Yangzhou, Jiangsu 225127, People's Republic of China*
[3]*Uni-enterprise (China) Holding Ltd., Kunshan, Jiangsu 215300, People's Republic of China*

(Submitted 6 March 2019 – Final revision received 9 July 2019 – Accepted 11 July 2019 – First published online 30 September 2019)

Abstract

Excessive intake of high-energy diets is an important cause of most obesity. The intervention of rats with high-fat diet can replicate the ideal animal model for studying the occurrence of human nutritional obesity. Proteomics and bioinformatics analyses can help us to systematically and comprehensively study the effect of high-fat diet on rat liver. In the present study, 4056 proteins were identified in rat liver by using tandem mass tag. A total of 198 proteins were significantly changed, of which 103 were significantly up-regulated and ninety-five were significantly down-regulated. These significant differentially expressed proteins are primarily involved in lipid metabolism and glucose metabolism processes. The intake of a high-fat diet forces the body to maintain physiological balance by regulating these key protein spots to inhibit fatty acid synthesis, promote fatty acid oxidation and accelerate fatty acid degradation. The present study enriches our understanding of metabolic disorders induced by high-fat diets at the protein level.

Key words: **High-fat diet: Proteomics: Bioinformatics: Lipid metabolism**

Changes in the structure of modern diets and excessive intake of high-fat, high-energy diets cause disorders in the metabolism of fats, proteins and carbohydrates. Excess energy is gradually accumulated in the body in the form of fat, which leads to obesity[1]. After the formation of obesity, it will further induce insulin resistance (IR), which in turn increases the incidence of the metabolic syndrome, diabetes, hypertension and CVD[2]. The liver plays a vital role in maintaining the body's carbohydrate, lipid and protein metabolism balance[3]. Obesity-related metabolic disorders are manifested in the liver, causing excessive deposition of fat in the liver cells, which can lead to fatty liver[4]. The pathogenesis of obesity is not fully understood. It is generally believed that obesity is mainly caused by the combination of genetic factors and environmental factors[5]. In addition, factors such as endocrine, metabolism and central nervous system are also involved in the pathogenesis of obesity[6].

Unlike traditional molecular biology techniques, proteomics enables researchers to define a global overview of protein expression in a specific physical or pathological state. In the present study, rats were treated with a high-fat diet to replicate an animal model with an obese phenotype similar to human obesity[7]. The effects of high-fat diet on rat liver protein expression were studied by tandem mass tag combined with LC-MS/MS. Bioinformatics analysis was used to further screen out the significant differential proteins that play a key role and to explore the mechanism of the body's response to high-fat diets.

Materials and methods

Animals and treatment

Eighteen healthy male Sprague–Dawley rats which were 5 weeks old and weighing about 150 g at the start of the experiment were purchased from Comparative Medical Center of Yangzhou University, Jiangsu, China. The animal experiments conformed the U.S. National Institutes of Health guidelines for the care and use of laboratory animals (NIH publication no. 85-23 Rev. 1985) and were approved by the Animal Care Committee of the Center for Disease Control and Prevention (Jiangsu, China). Then, rats were randomly divided into a control group (C) and high-fat diet group (HF) (*n* 9). The control group

Abbreviations: GO, gene ontology; HF, high-fat diet group; IR, insulin resistance; KEGG, Kyoto Encyclopedia of Genes and Genomes; UGT, UDP-glucuronosyltransferase.

* **Corresponding author:** Y. Huang, email yjhuang@yzu.edu.cn
† These authors contributed equally to this work and should be regarded as co-first authors.

Table 1. Composition of the diets

Diet	Ingredient	Content (%, w/w)	Total energy (kJ/100g)
Low-fat diet	Flour	20	690·36
	Rice flour	10	
	Maize	20	
	Drum skin	26	
	Soya material	20	
	Fishmeal	2	
	Bone flour	2	
High-fat diet	Lard	10	1548·08
	Egg powder	10	
	Cholesterol	1	
	Bile salts	0·2	
	Low-fat diet	78·8	

was fed a low-fat diet (Table 1). The HF was fed a high-fat diet (Table 1) for 8 weeks. All rats were housed under a 12 h light–12 h dark cycle in a controlled room with a temperature of 23°C and a humidity of 50 % and allowed free access to food and water. After 8 weeks, rats underwent 12 h of fasting prior to being anaesthetised and dissected. All rats were euthanised at the anoestrus period, following anaesthesia under 1 % sodium pentobarbital. Livers were removed and stored at 4 and −80°C for subsequent analyses.

Compliance with ethics guidelines

All institutional and national guidelines for the care and use of laboratory animals were followed.

Haematoxylin–eosin staining

Liver samples were fixed in 4 % paraformaldehyde for more than 48 h, followed by sectioning after embedding with paraffin. The paraffin section was stained by routine haematoxylin–eosin methods.

Protein extraction and normalisation

SDT buffer (4 % (w/v) SDS, 0·1 M DL-dithiothreitol, 100 mM Tris/HCl, pH 7·6) was added to the liver sample and transferred to 2 ml tubes with quartz sand (another 1/4 inch ceramic bead MP 6540-424 for tissue samples). The lysate was homogenised by an MP homogeniser (24 × 2, 6·0 m/s, 60 s, twice). The homogenate was sonicated and then boiled for 15 min. After centrifuged at 14 000 ***g*** for 40 min, the supernatant was filtered with 0·22 μm filters. The filtrate was quantified with the Bicinchoninic Acid Protein Assay Kit (Bio-Rad). The sample was stored at −80°C. Equivalent amounts of protein from each of the three different rats were pooled to generate three protein samples for each group.

SDS-PAGE separation

A quantity of 20 μg of proteins for each sample was mixed with 5× loading buffer and boiled for 5 min. The proteins were separated on 12·5 % SDS-PAGE gel (constant current 14 mA, 90 min). Protein bands were visualised by Coomassie Blue R-250 staining.

Filter-aided sample preparation digestion

A quantity of 200 μg of proteins for each sample was incorporated into 30 μl SDT buffer (4 % SDS, 100 mM dithiothreitol, 150 mM Tris-HCl, pH 8·0). The detergent, dithiothreitol and other low-molecular-weight components were removed using UA buffer (8 M urea, 150 mM Tris-HCl, pH 8·0) by repeated ultrafiltration (microcon units, 10 kDa). Then, 100 μl iodoacetamide (100 mM iodoacetamide in UA buffer) was added to block reduced cysteine residues, and the samples were incubated for 30 min in darkness. The filters were washed with 100 μl UA buffer three times and then with 100 μl 100 mM triethylammonium bicarbonate (TEAB) buffer twice. Finally, the protein suspensions were digested with 4 μg trypsin (Promega) in 40 μl TEAB buffer overnight at 37°C, and the resulting peptides were collected as a filtrate. The peptide content was estimated by UV light spectral density at 280 nm using an extinction coefficient of 1·1 of 0·1 % (g/l) solution which was calculated on the basis of the frequency of tryptophan and tyrosine in vertebrate proteins

Tandem mass tag labelling

The peptide mixture (100 μg) of each sample was labelled using a tandem mass tag reagent according to the manufacturer's instructions (Thermo Fisher Scientific).

Peptide fractionation with high pH reversed phase

A Pierce high pH reversed-phase fractionation kit (Thermo Scientific) was used to fractionate tandem mass tag-labelled digest samples into ten fractions by an increasing acetonitrile step-
gradient elution according to the instructions.

Mass spectrometry

HPLC. Each fraction was injected for nanoLC-MS/MS analysis. The peptide mixture was loaded onto a reversed-phase trap column (Thermo Scientific Acclaim PepMap100, 100 μm × 2 cm, nanoViper C18) connected to the C18-reversed-phase analytical column (Thermo Scientific Easy Column, 10 cm long, 75 μm inner diameter, 3 μm resin) in buffer A (0·1 % formic acid) and separated with a linear gradient of buffer B (84 % acetonitrile and 0·1 % formic acid) at a flow rate of 300 nl/min controlled by IntelliFlow technology.

1·5 h gradient: 0–55 % buffer B for 80 min, 55–100 % buffer B for 5 min, hold in 100 % buffer B for 5 min.

LC-MS/MS analysis. LC-MS/MS analysis was performed on a Q Exactive MS (Thermo Scientific) that was coupled with Easy nLC (Proxeon Biosystems, now Thermo Fisher Scientific) for 90 min (determined by project proposal). The MS was operated in positive ion mode. Mass spectometry data were acquired using a data-dependent top-ten method dynamically choosing the most abundant precursor ions from the survey scan (300–1800 m/z) for higher-energy C-trap dissociation (HCD) fragmentation. Automatic gain control target was set to 3e6 and maximum inject time to 10 ms. Dynamic exclusion duration was 40·0 s. Survey scans were acquired at a resolution of 70 000 at m/z 200, the resolution for HCD spectra was set to 35 000 at m/z 200 and isolation

British Journal of Nutrition

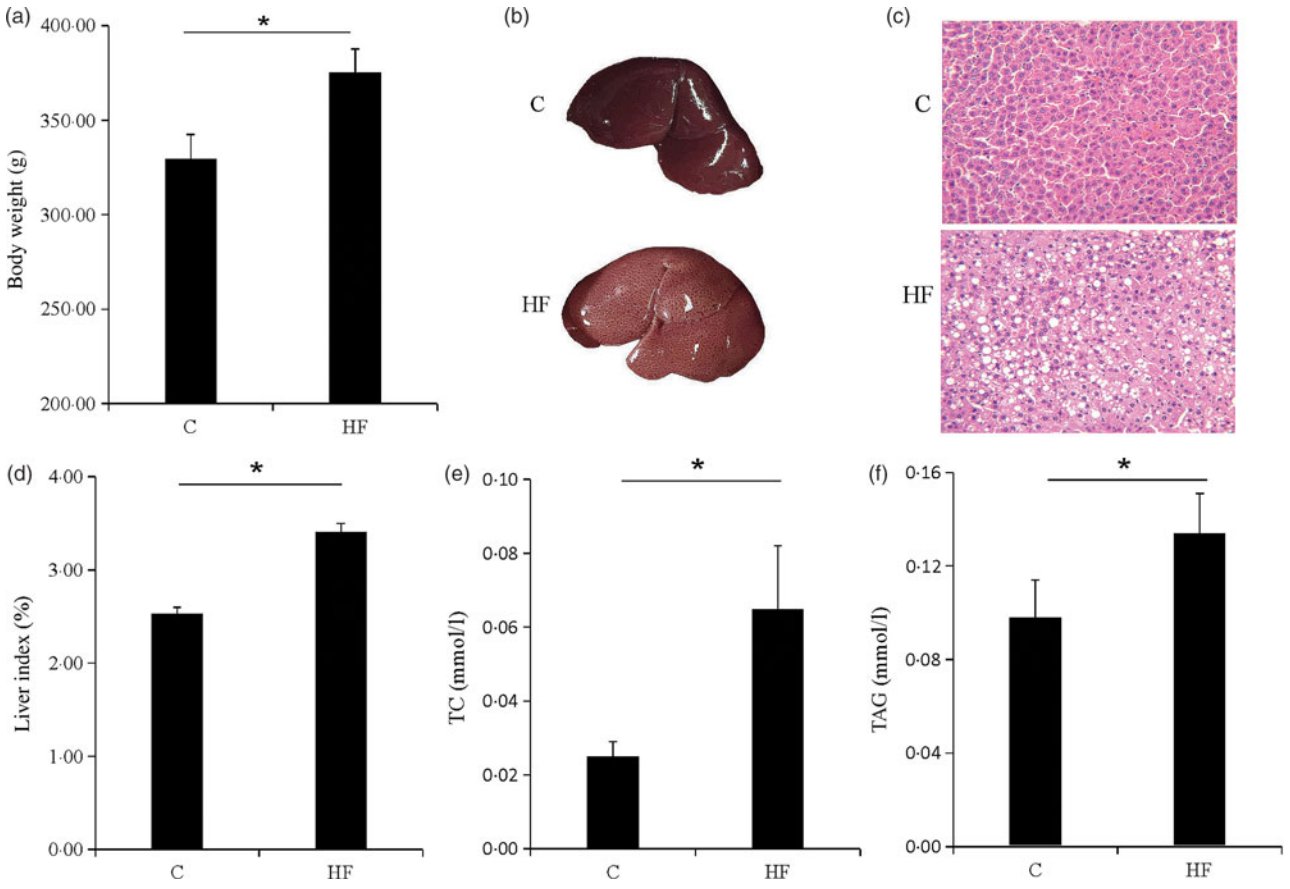

Fig. 1. Obesity and liver steatosis. (a) Body weight of rats. (b) Images of representative rat livers. (c) Haematoxylin–eosin staining of livers. (d) Liver index of livers. (e and f) Total cholesterol (TC) and TAG of livers. Values are means (n 9), with their standard errors represented by vertical bars. * $P < 0{\cdot}05$. C, control group; HF, high-fat diet group.

width was 2 *m/z*. Normalised collision energy was 30 eV, and the underfill ratio, which specifies the minimum percentage of the target value likely to be reached at maximum fill time, was defined as 0·1 %. The instrument was run with peptide recognition mode enabled.

Data analysis

MS/MS spectra were searched using MASCOT engine (Matrix Science; version 2.2) embedded into Proteome Discoverer 1.4 (online Supplementary Table S1).

Bioinformatics analysis

Hierarchical clustering. The protein-relative expression data were selected for hierarchical clustering analysis, and Cluster 3.0 and the Java Treeview software were used. Euclidean distance algorithm for measuring similarity and average linkage clustering algorithm (clustering uses the centroids of the observations) for clustering were selected when performing hierarchical clustering.

Gene ontology functional annotation. The protein sequences of differentially expressed proteins were in batches retrieved from UniProtKB database (Release 2016_10) in FASTA format. The retrieved sequences were locally searched against SwissProt database using the NCBI BLAST + client software (ncbi-blast-2.2.28+-win32.exe) to find homologue sequences, from which the functional annotation can be transferred to the studied sequences. In this work, the top ten blast hits with E-value less than 1*e*-3 for each query sequence were retrieved and loaded into Blast2GO (version 3.3.5) for gene ontology (GO) mapping and annotation. In this work, an annotation configuration with an E-value filter of 1*e*-6, default gradual EC weights, a GO weight of 5 and an annotation cut-off of 75 was chosen. Un-annotated sequences were then re-annotated with more permissive parameters. The sequences without BLAST hits and un-annotated sequences were then selected to go through an InterProScan against EBI databases to retrieve functional annotations of protein motifs and merge the InterProScan GO terms to the annotation set. The GO annotation results were plotted by R scripts.

Kyoto Encyclopedia of Genes and Genomes pathway annotation. The FASTA protein sequences of differentially changed proteins were blasted against the online Kyoto Encyclopedia of Genes and Genomes (KEGG) database (http://geneontology.org/) to retrieve their KEGG orthology and were subsequently mapped to pathways in KEGG. The corresponding KEGG pathways were extracted.

Table 2. Differentially expressed proteins (top 20)

Accession	Description	High-fat diet group:control group	*P*
Q62818	Translation initiation factor eIF-2B subunit β, Eif2b2	2·16653058	0·000718203
Q5XIJ6	BRISC and BRCA1-A complex member 1, Babam1	2·047810457	0·003061915
Q5U2U5	Perilipin, Plin2	2·013776015	$5{\cdot}94017 \times 10^{-5}$
P51647	Retinal dehydrogenase 1, Aldh1a1	1·840092428	$3{\cdot}4716 \times 10^{-5}$
P19225	Cytochrome P450 2C70, Cyp2c70	1·808583525	$9{\cdot}953 \times 10^{-7}$
Q5U1W1	Apo L, 3, Apol3	1·754127158	0·048575846
P07687	Epoxide hydrolase 1, Ephx1	1·732555816	$3{\cdot}21041 \times 10^{-6}$
P07871	Peroxisomal 3-ketoacyl-CoA thiolase B, Acaa1b	1·728987207	0·001173721
M0R5Y4	Myotilin-like, LOC100909868	1·682931624	0·003932265
P46418	Glutathione S-transferase α-5, Gsta5	1·676939556	0·000423909
Q6AYS8	Oestradiol 17-β-dehydrogenase 11, Hsd17b11	1·652588897	$1{\cdot}39328 \times 10^{-5}$
P05183	Cytochrome P450 3A2, Cyp3a2	1·588862955	$1{\cdot}98411 \times 10^{-5}$
G3V9D8	Carboxylic ester hydrolase, LOC108348093	1·583811454	$1{\cdot}61313 \times 10^{-6}$
D3ZHL7	Prospero homeobox 2, Prox2	1·558385759	0·001853077
B2RZ37	Receptor expression-enhancing protein 5, Reep5	1·539226349	$2{\cdot}31705 \times 10^{-5}$
A0A0G2K9M5	TBC1 domain family member 8B, Tbc1d8b	1·538767753	0·015112944
Q6AXY8	Dehydrogenase/reductase (SDR family) member 1, Dhrs1	1·536302694	$2{\cdot}83349 \times 10^{-5}$
Q06884	Cytochrome P450, Cyp3a23/3a1	1·511835628	0·000147063
P38918	Aflatoxin B1 aldehyde reductase member 3, Akr7a3	1·494791392	0·0002348
Q64550	UDP-glucuronosyltransferase 1-1, Ugt1a1	1·493772264	$8{\cdot}17548 \times 10^{-5}$
P55053	Fatty acid-binding protein, epidermal, Fabp5	0·663932034	0·000354964
M0R5W4	Mevalonate kinase, Mvk	0·658233192	0·000188818
P13221	Aspartate aminotransferase, cytoplasmic, Got1	0·657320844	0·000578741
A0A0G2JSK9	Betaine–homocysteine S-methyltransferase 1, Bhmt	0·652554713	0·006650038
D3ZLH3	Uncharacterised protein, D3ZLH3	0·641095034	0·008887422
P17425	Hydroxymethylglutaryl-CoA synthase, cytoplasmic, Hmgcs1	0·637975371	$2{\cdot}28098 \times 10^{-5}$
A0A0G2K5L6	Acetyl-CoA carboxylase β, Acacb	0·620561456	0·000727809
Q499N5	Acyl-CoA synthetase family member 2, mitochondrial, Acsf2	0·611555822	$2{\cdot}62666 \times 10^{-5}$
Q5XI22	Acetyl-CoA acetyltransferase, cytosolic, Acat2	0·60115063	0·002030085
A0A0G2K5E7	ATP-citrate synthase, Acly	0·592843177	0·000177244
Q62967	Diphosphomevalonate decarboxylase, Mvd	0·54143832	0·000104039
A0A0G2JYC0	Sulfotransferase, Sult2a1	0·5315533	0·002870979
P24008	3-Oxo-5-α-steroid 4-dehydrogenase 1, Srd5a1	0·525394422	0·005337289
H2BF30	Fatty acid desaturase 1, Fads1	0·521494666	0·000850261
Q5BK21	Transmembrane 7 superfamily member 2, Tm7sf2	0·521209242	$3{\cdot}53412 \times 10^{-5}$
Q64654	Lanosterol 14-α demethylase, Cyp51a1	0·48298834	0·001880132
O35760	Isopentenyl-diphosphate delta-isomerase 1, Idi1	0·480183314	0·00060506
P12785	Fatty acid synthase, Fasn	0·473020925	0·001360118
F1LND7	Farnesyl pyrophosphate synthase, Fdps	0·446203424	0·000196497
Q02769	Squalene synthase, Fdft1	0·440502843	0·001587728

Functional enrichment analysis. To further explore the impact of differentially expressed protein in cell physiological process and discover internal relations between differentially expressed proteins, enrichment analysis was performed. GO enrichment on three ontologies (biological process, molecular function and cellular component) and KEGG pathway enrichment analyses were applied based on the Fisher's exact test, considering the whole quantified protein annotations as background data set. Benjamini–Hochberg correction for multiple testing was further applied to adjust derived *P* values. Only functional categories and pathways with *P* values under a threshold of 0·05 were considered as significant.

Results

Obesity and liver steatosis

The symptoms of obesity were observed in the HF. The body weight of the HF was significantly increased ($P < 0{\cdot}05$) (Fig. 1(a)). The liver of the rat was swollen and brittle (Fig. 1(b)), and haematoxylin–eosin staining showed that the structure of the liver cells was destroyed and a large number of fat vacuoles were observed (Fig. 1(c)). Liver index, liver TAG and total cholesterol were significantly increased ($P < 0{\cdot}05$) (Fig. 1(d)–(f)). The high-fat diet caused rat liver fat accumulation, and the lipid metabolism balance in the liver was destroyed.

Screening of differentially expressed proteins

A total of 4056 proteins were identified by MS. Proteins that conformed to the following screening criteria were deemed as differentially expressed: 1·2-fold for up-regulated proteins and 0·83-fold for down-regulated proteins ($P < 0{\cdot}05$). A total of 198 differentially expressed proteins (103 increased, ninety-five decreased) were found between HF and C (Table 2, online Supplementary Table S2).

Hierarchical clustering

Hierarchical clustering results were expressed as a tree heat map (Fig. 2). The differentially expressed proteins screened in the present study can effectively separate the HF from the C. The

hierarchical clustering analysis thus supported that the differentially expressed proteins screened out were reasonable.

Gene ontology functional annotation analysis

The most prevalent biological processes were biological_process (178), cellular process (164), single-organism cellular process (161) and metabolic process (150). The most prevalent cellular components were located in the cellular_component (194), cell (183), cell part (183) and intracellular (177). The most predominant molecular functions were molecular_function (182), binding (13) and catalytic activity (127) (Fig. 3, online Supplementary Table S3).

In addition, lipid metabolic process, monocarboxylic acid metabolic process, organic acid metabolic process, oxoacid metabolic process, carboxylic acid metabolic process and other important biological processes changed significantly. Oxidoreductase activity, catalytic activity, steroid hydroxylase activity, carboxylic ester hydrolase activity, glucuronosyltransferase activity and other molecular function change significantly. Acetyl-CoA carboxylase complex, microbody, peroxisome, endoplasmic reticulum, lipid particle and other positioning proteins changed significantly (Fig. 4).

Kyoto Encyclopaedia of Genes and Genomes pathway analysis

A total of 143 KEGG pathways (online Supplementary Table S4) had been enriched, and forty important KEGG pathways (Table 3) changed significantly such as retinol metabolism, steroid hormone biosynthesis, PPAR signalling pathway, fatty acid metabolism, IR and so on.

Discussion

The liver is the main site of lipid metabolism. On the one hand, the liver takes up NEFA from the blood to synthesise TAG. On the other hand, the liver secretes endogenous TAG synthesised into the blood, thereby transporting it to the extrahepatic tissues. The two are in a dynamic balance. Once the balance is destroyed, it will cause fat to accumulate in the liver. Studies have reported that high-fat diet has an important impact on the lipid metabolism process in rat liver[8]. The present study further validates this view and discovers some new differentially expressed proteins. GO functional enrichment analysis revealed significant changes in the multiple biological processes associated with lipid metabolism, and the KEGG analysis found significant changes in the pathways of fatty acid synthesis, degradation and metabolism. The high-fat diet caused significant changes in proteins such as peroxisomal bifunctional enzyme (Ehhadh), 3-ketoacyl-CoA thiolase B (Acaa1b), 3-ketoacyl-CoA thiolase A (Acaa1a), Acetyl-CoA carboxylase 1 (Acaca1) and Acetyl-CoA acetyltransferase (Acat) on these pathways. Ehhadh is part of the classical peroxisomal fatty acid β-oxidation pathway. It is a downstream target gene of PPARα and regulates its gene expression through PPARα to participate in intracellular lipid metabolism[9]. Overexpression of Ehhadh leads to a decrease in intracellular fatty acid content[10]. Acaa1a and Acaa1b are two

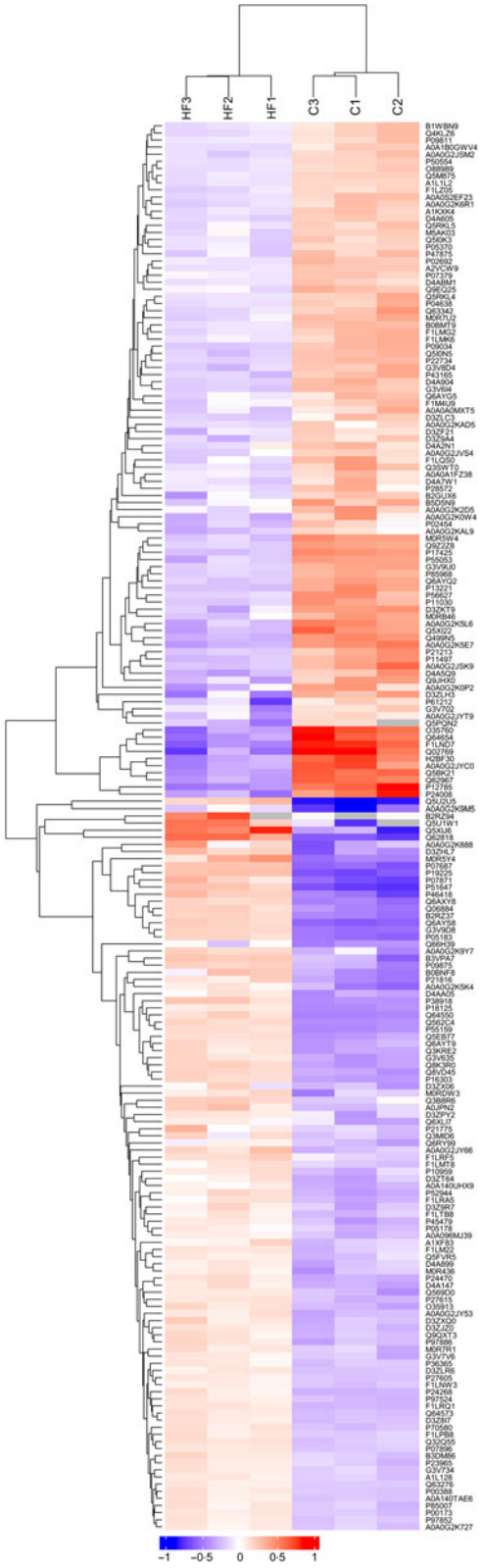

Fig. 2. Hierarchical clustering. X-coordinates represent samples and Y-coordinates differentially expressed proteins. Log_2-expression of differentially expressed proteins in tested samples is displayed in different colours in the heat map, with red representing up-regulation and green indicating down-regulation.

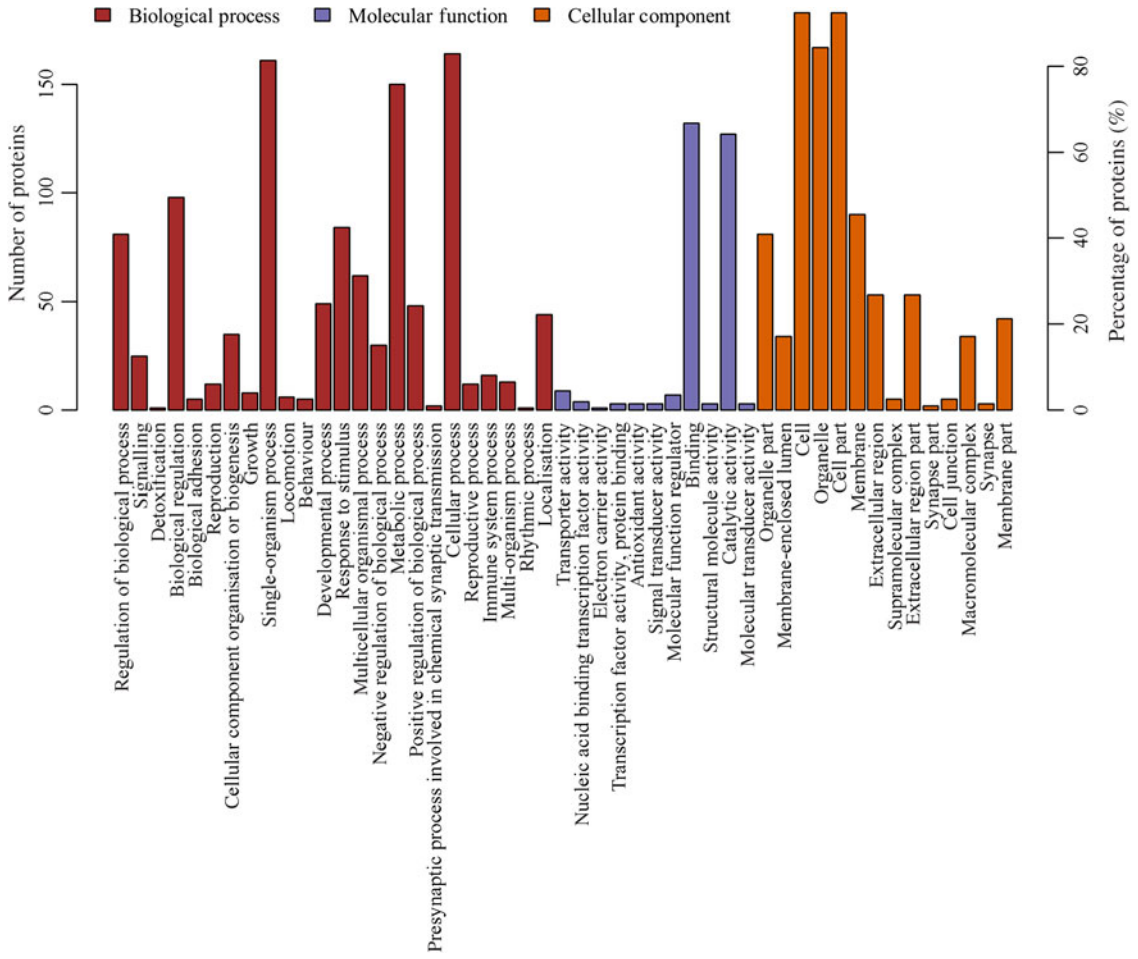

Fig. 3. Gene ontology (GO) functional annotation analysis of the differentially expressed proteins. X-coordinates represent GO functional annotations and Y-coordinates represent the number and percentage of proteins.

different peroxisomal 3-ketoacyl-CoA thiolases for very-long-straight-chain fatty acids[11]. There are four enzymatic steps in each cycle of peroxisomal β-oxidation: oxidation, hydration, dehydrogenation and thiolytic cleavage. Acaa1a and Acaa1b catalyse the final step in the peroxisomal β-oxidation of straight-chain acyl-CoAs[12–14]. Acaca1 is a rate-limiting enzyme for fatty acid synthesis which catalyses the first step of fatty acid synthesis. Acaca1 is mainly found in adipose tissue and liver, and its main function is to produce malonyl-CoA as an activated two-carbon unit for fatty acid synthesis[15]. Acat is a membrane protein located on the endoplasmic reticulum of cells and is the rate-limiting enzyme for the synthesis of cholesterol and long-chain fatty acyl-CoA[16]. In the present study, the expression of Ehhadh, Acaa1a and Acaa1b was significantly up-regulated and the expression levels of Acaca1 and Acat were significantly down-regulated in the HF. It indicates that after ingesting a high-fat diet, the body inhibited fatty acid synthesis, promoted the oxidation process of fatty acids in peroxisomal and accelerated the degradation of fatty acids in order to maintain lipid metabolism balance.

The liver is the main target organ for insulin action[17]. IR is the basis for the link between obesity and most of its associated metabolic disorders, including type 2 diabetes, fatty liver disease, dyslipidaemia and CVD, and is usually only manifested in the clinical manifestations of obesity[18]. The KEGG analysis revealed significant changes in the IR pathway and insulin signalling pathway. Proteins such as acetyl-CoA carboxylase β (Acacb), phosphoenolpyruvate carboxykinase and glycogen phosphorylase were significantly down-regulated in the HF. Acetyl-CoA carboxylase β plays an important role in the regulation of lipid synthesis and oxidation in lipid metabolism and has a close relationship with insulin[19]. Insulin can restore activity by dephosphorylation of Acacb by the action of protein phosphatase. Acetyl-CoA carboxylase β reduces the oxidation of fatty acids and increases the accumulation of fat in the body, which in turn increases the body's IR[20]. Phosphoenolpyruvate carboxykinase is a key rate-limiting enzyme in gluconeogenesis that catalyses the conversion of oxaloacetate to phosphoenolpyruvate[21]. Glycogen phosphorylase is a key enzyme in glycogen metabolism[22]. By inhibiting the protein expression of Acacb, phosphoenolpyruvate carboxykinase and glycogen phosphorylase, the body inhibits the gluconeogenesis pathway and enhances catabolism and increases the sensitivity of hepatic insulin after a high-fat diet.

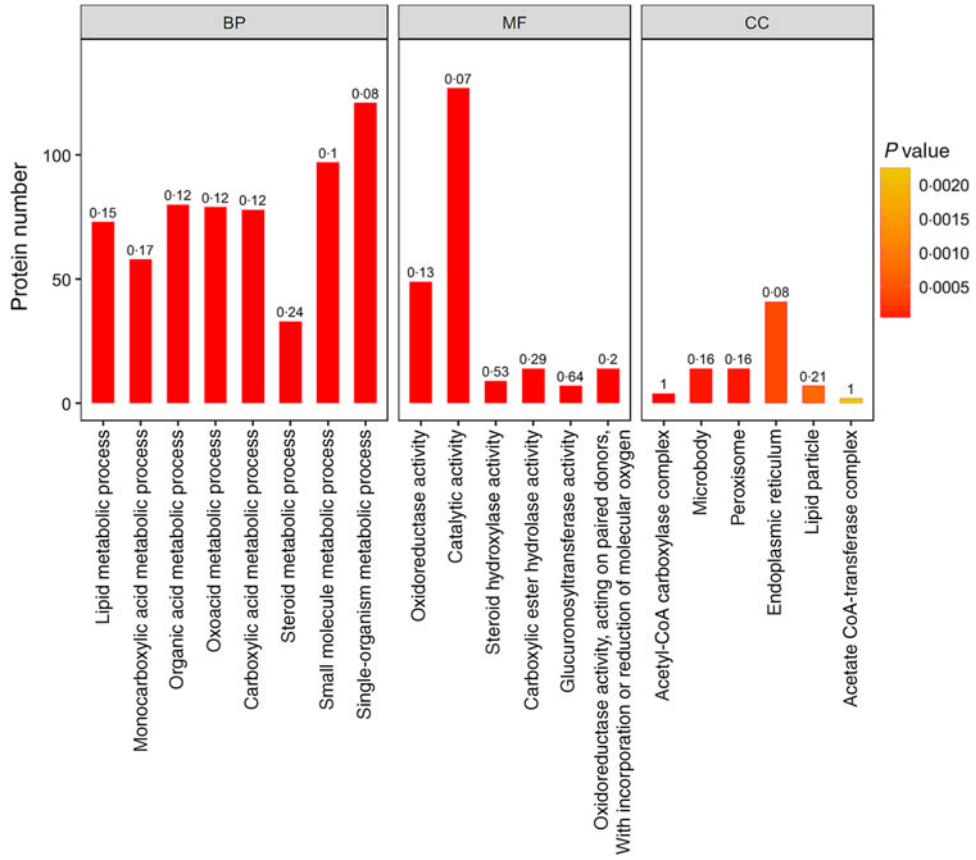

Fig. 4. Gene ontology (GO) functional enrichment analysis of the differentially expressed proteins (top 20). The bar graph colour indicates the significance of the enriched GO functional classification, and the *P* value is calculated based on Fisher's exact test. The colour gradient represents the magnitude of the *P* value. The closer to the red, the smaller the *P* value, and the higher the significance level of the corresponding GO functional category enrichment. The label above the bar graph shows the enrichment factor (rich Factor ≤ 1), and the enrichment factor indicates the ratio of the number of differentially expressed proteins annotated to a GO functional category to the number of all identified proteins annotated to the GO functional category. BP, biological processes; MF, molecular functions; CC, cellular components.

At the same time, the liver is also the main site of amino acid metabolism. Amino acids are decomposed into α-keto acids by deamination. Part of α-keto acid produces glucose through gluconeogenesis, and some α-keto acids participate in fat metabolism to produce fat[23]. The KEGG pathway analysis revealed significant changes in a variety of amino acid metabolic pathways such as glycine, serine and threonine metabolism, cysteine and methionine metabolism, alanine, aspartate and glutamate metabolism and tyrosine metabolism. In these pathways, aspartate aminotransferase cytoplasmic (GOT1), argininosuccinate synthase (ASS1), L-serine dehydratase/L-threonine deaminase (Sds) and 4-aminobutyrate aminotransferase (Abat) were significantly down-regulated. We speculate that the body inhibits gluconeogenesis and fat metabolism by inhibiting partial amino acid metabolism.

The PPAR signalling pathway plays an important role in regulating lipid metabolism and glucose metabolism. The KEGG pathway analysis also found significant changes in the PPAR signalling pathway. Peroxisome proliferator-activated receptors consist of three receptor subtypes, PPAR-α, β/δ and γ. Peroxisome proliferator-activated receptor-α plays a key role in regulating fatty acid uptake, β-oxidation, ketone synthesis, bile acid synthesis and TAG transport[24,25]. Peroxisome proliferator-activated receptor-β/δ is involved in the regulation of mitochondrial metabolism and fatty acid β-oxidation[26,27]. Peroxisome proliferator-activated receptor-γ regulates adipocyte differentiation and lipid metabolism[28]. In the present study, a total of fourteen PPAR-related proteins were significantly changed (Fig. 5). The body inhibits the expression of fatty acid-binding protein by increasing the expression of platelet glycoprotein 4 (FATCd36). Cholesterol metabolism-related protein (cholesterol 7-α-mono-oxygenase (CYP7A1)) and fatty acid oxidation-related proteins (3-ketoacyl-CoA thiolase B (thiolase B/Acaa1b) and acyl-CoA oxidase) were significantly up-regulated. Lipid transport-related protein (apo A-II (Apoa2)) and fatty acid transport-related proteins (acyl-CoA-binding protein and liver fatty acid-binding protein (Fabp1)) were significantly down-regulated. In turn, it affects lipid metabolism and accelerates fatty acid degradation. In addition, perilipin was significantly up-regulated to promote adipocyte differentiation, and Phosphoenolpyruvate carboxykinase was significantly down-regulated to inhibit gluconeogenesis.

As the most important detoxification organ, the liver contains most of the phase I and phase II metabolic enzymes, which affect the metabolism of endogenous and exogenous substances[29]. KEGG pathway analysis revealed that metabolism of xenobiotics

Table 3. Significantly changed pathways of high-fat diet group:control group

Map_ID	Map_Name	Test	Test_Seq
map00830	Retinol metabolism	21	P19225 P05183 F1LRQ1 P51647 Q64550 D3ZLR6 Q8VD45 Q06884 P24470 G3V635 A1L128 D4A147 P09875 P97886 F1LM22 F1LTB8 G3V7V6 P05178 A0A0G2K5K4 A1XF83 D4ABM1
map05204	Chemical carcinogenesis	21	P19225 P07687 P05183 Q64550 D3ZLR6 Q8VD45 Q06884 P24470 G3V635 P46418 A1L128 D4A147 P09875 P97886 F1LM22 F1LTB8 P05178 A0A0G2K5K4 A1XF83 D4ABM1 A0A0G2JYC0
map00140	Steroid hormone biosynthesis	20	P19225 P18125 P05183 Q64550 D3ZLR6 Q8VD45 Q06884 P24470 G3V635 D4A147 P09875 P97886 F1LM22 F1LTB8 P05178 A0A0G2K5K4 A1XF83 P22734 D4ABM1 P24008
map00983	Drug metabolism – other enzymes	17	G3V9D8 P16303 Q8K3R0 Q64550 Q32Q55 P27605 D3ZLR6 Q8VD45 D4A147 P09875 P97886 F1LM22 A0A0G2JY66 F1LTB8 P10959 D3ZXQ0 A1XF83
map04976	Bile secretion	15	P07687 P18125 Q64550 D3ZLR6 Q8VD45 Q63276 O35913 D4A147 P09875 P97886 F1LM22 F1LTB8 A1XF83 A0A0G2JYC0 P56627
map03320	PPAR signalling pathway	14	P18125 P07896 Q5U2U5 F1LNW3 P97524 A0A096MJ39 P07871 P21775 P17425 P55053 P02692 P07379 P11030 P04638
map00980	Metabolism of xenobiotics by cytochrome P450	14	P07687 Q64550 D3ZLR6 Q8VD45 P38918 P46418 A1L128 D4A147 P09875 P97886 F1LM22 F1LTB8 A1XF83 A0A0G2JYC0
map00982	Drug metabolism – cytochrome P450	13	F1LRQ1 Q64550 D3ZLR6 Q8VD45 P46418 A1L128 D4A147 P09875 P36365 P97886 F1LM22 F1LTB8 A1XF83
map01200	Carbon metabolism	12	P07896 G3V9U0 P85968 Q5I0N5 P13221 O88989 Q5XI22 P05370 Q4KLZ6 D4A5Q9 F1LMK6 B1WBN9
map00053	Ascorbate and aldarate metabolism	9	Q64550 D3ZLR6 Q8VD45 D4A147 P09875 P97886 F1LM22 F1LTB8 A1XF83
map00040	Pentose and glucuronate interconversions	9	Q64550 D3ZLR6 Q8VD45 D4A147 P09875 P97886 F1LM22 F1LTB8 A1XF83
map00860	Porphyrin and chlorophyll metabolism	9	Q64550 D3ZLR6 Q8VD45 D4A147 P09875 P97886 F1LM22 F1LTB8 A1XF83
map01212	Fatty acid metabolism	9	P07896 A0A140TAE6 P07871 P45479 P21775 H2BF30 P11497 P12785 Q5XI22
map04146	Peroxisome	9	P07896 F1LNW3 Q63276 P97524 P97852 P07871 P21775 M0R5W4 Q5I0N5
map00591	Linoleic acid metabolism	8	P19225 P05183 Q06884 P24470 G3V635 P05178 A0A0G2K5K4 D4ABM1
map00640	Propanoate metabolism	7	P07896 G3V9U0 P50554 A0A0G2K5L6 P11497 Q5XI22 Q6AYG5
map00620	Pyruvate metabolism	7	G3V9U0 A0A0G2K5L6 P07379 O88989 P11497 Q5XI22 B1WBN9
map00280	Valine, leucine and isoleucine degradation	7	P07896 F1LRQ1 P07871 P21775 P17425 P50554 Q5XI22
map00900	Terpenoid backbone biosynthesis	6	P17425 Q62967 M0R5W4 F1LND7 O35760 Q5XI22
map00270	Cysteine and methionine metabolism	6	P21816 P13221 O88989 F1LMG2 A0A0G2JSK9 F1LMK6
map00260	Glycine, serine and threonine metabolism	6	Q5I0N5 Q5RKL4 D4A5Q9 A0A0G2JSK9 F1LMK6 Q63342
map00071	Fatty acid degradation	6	P07896 A1L128 P07871 P23965 P21775 Q5XI22
map04910	Insulin signalling pathway	6	A0A0G2K5L6 P07379 P11497 P12785 P09811 B1WBN9
map00100	Steroid biosynthesis	5	Q9Z2Z8 Q5BK21 A1KXK4 Q02769 Q64654
map00120	Primary bile acid biosynthesis	5	P18125 F1LNW3 Q63276 P97852 D3ZPY2
map00650	Butanoate metabolism	5	P07896 Q6AYT9 P17425 P50554 Q5XI22
map00250	Alanine, aspartate and glutamate metabolism	5	P50554 Q5I0N5 P09034 P13221 A0A0S2EF23
map04931	Insulin resistance	5	P97524 A0A096MJ39 A0A0G2K5L6 P07379 P09811
map00480	Glutathione metabolism	5	P46418 Q9QXT3 M0RDW3 P85968 P05370
map00220	Arginine biosynthesis	4	P09034 D4A904 P13221 A0A0S2EF23
map00350	Tyrosine metabolism	4	F1LRQ1 A1L128 P22734 P13221
map01040	Biosynthesis of unsaturated fatty acids	4	Q63276 P07871 P21775 H2BF30
map00630	Glyoxylate and dicarboxylate metabolism	4	Q5I0N5 O88989 Q5XI22 D4A5Q9
map00430	Taurine and hypotaurine metabolism	3	Q63276 P21816 B3VPA7
map00061	Fatty acid biosynthesis	3	A0A0G2K5L6 P11497 P12785
map04964	Proximal tubule bicarbonate reclamation	3	P07379 O88989 A0A0S2EF23
map04975	Fat digestion and absorption	3	A0A096MJ39 P02692 Q5XI22
map00592	α-Linolenic acid metabolism	2	P07871 P21775
map00524	Neomycin, kanamycin and gentamicin biosynthesis	2	A0A0G2K5L6 P11497
map00072	Synthesis and degradation of ketone bodies	2	P17425 Q5XI22

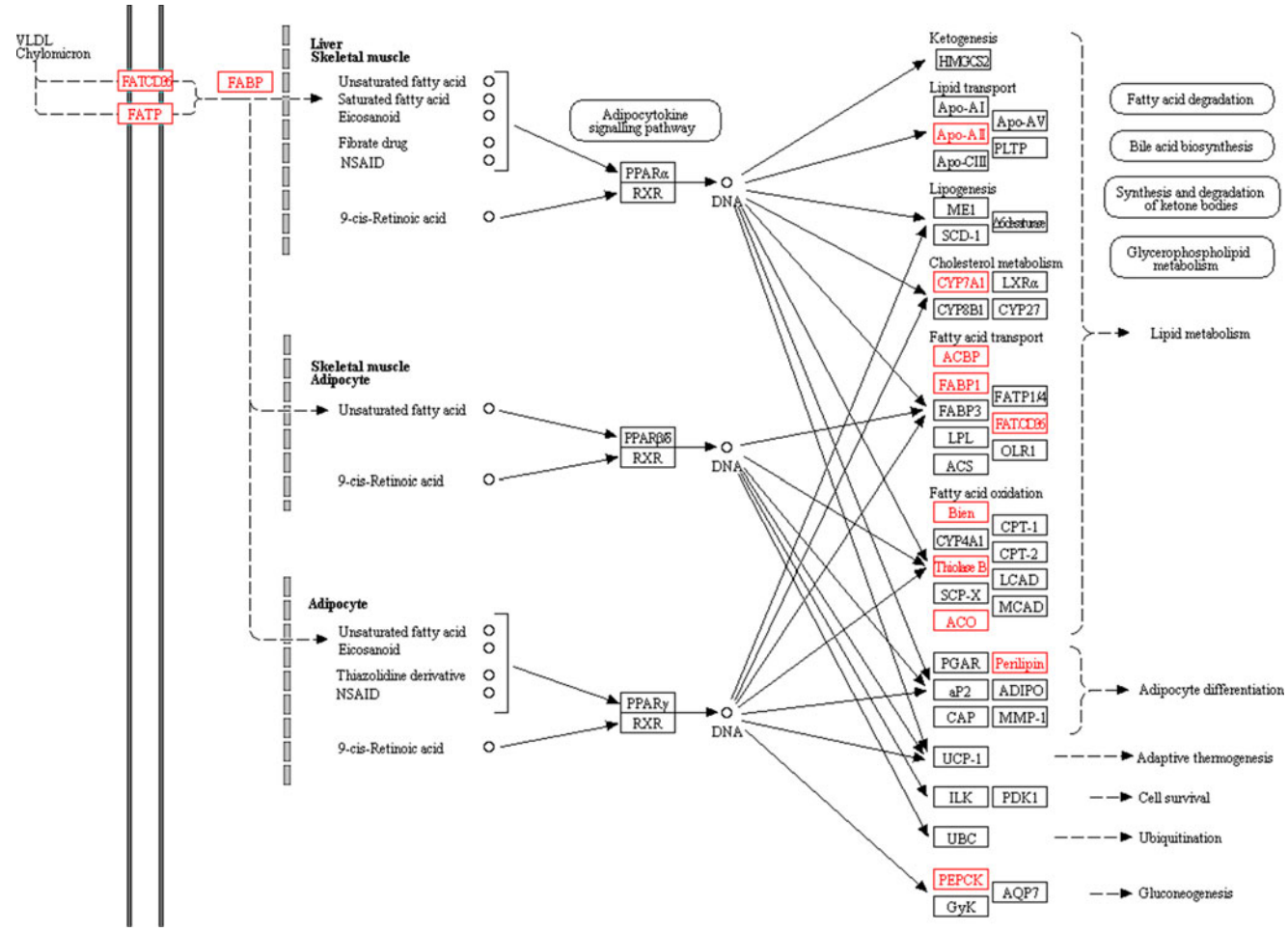

Fig. 5. PPAR signalling pathway. All differentially expressed proteins involved in this pathway are identified by red borders and fonts. Small circles represent small molecule metabolites, and large round boxes represent other pathways.

by cytochrome P450, drug metabolism – cytochrome P450, drug metabolism – other enzymes, steroid hormone biosynthesis and other pathways had changed significantly. The most important enzymes involved in these metabolisms were cytochrome P450 (CYP450) and UDP-glucuronosyltransferase (UGT). CYP450 is an enzyme system involved in phase I metabolism[30]. The metabolism of exogenous compounds (drugs, environmental pollutants, carcinogens, etc.) and endogenous compounds (steroid hormones, cholesterol, fatty acids, etc.) is mainly catalysed by CYP450[31]. The protein expression of CYP2C70, CYP7A1, CYP3A2, CYP3A23/3A1, CYP2C23, CYP3A18, CYP2C6 and CYP3A9 in the HF was significantly up-regulated in the present study. The KEGG pathway analysis revealed that these significant differential proteins are primarily involved in the steroid hormone biosynthesis pathway and the retinol metabolic pathway. This suggests that a high-fat diet can induce the expression of part of CYP450 in the liver, thereby promoting the metabolism of steroid hormones and retinol. The uronic acid-binding reaction is an important phase II metabolic pathway *in vivo* and mainly catalysed by UGT. UGT is a type of microsomal glycoprotein on the endoplasmic reticulum. When the liver lacks UGT, the liver's detoxification function of endogenous compounds (bilirubin, bile acids, thyroid hormones, and steroids) and exogenous compounds (drugs) will be affected, which in turn causes liver cell to be damaged[32]. In the present study, the protein expression of UGT1A1, UGT2B15, UGT1A5, UGT2A3, UGT1, UGT2B (F1LM22), UGT (RGD1559459), UGT2B (A1XF83) and UGT2B1 in the HF was significantly up-regulated. It indicated that the intake of high-fat diet had a certain induction effect on the expression of UGT. The body accelerates the biotransformation of bile acids, steroids and hormones by increasing the expression of UGT, so as to avoid damage to the liver caused by poisons. Studies had shown that in the liver damage state of liver fibrosis and early liver cirrhosis, the expression of UGT in rat liver was up-regulated[33], which may also indicate the occurrence of early liver fibrosis in the HF.

In addition, the phase I metabolic enzyme carboxylic ester hydrolase/carboxylesterase (Ces (LOC108348093), Ces1d (P16303), Ces2a, Ces2h, Ces1d (A0A0G2JY66), Ces1c and Ces2g), and phase II metabolic enzyme glutathione S-transferase *α*-5 (Gsta5) and N-acetyltransferase (Nat8 and Nat8f2) were significantly up-regulated. It showed the induction of metabolic enzymes by high-fat diet to promote liver metabolism.

The present study performed proteomic approaches and analszed the changes from a macro perspective. In future research, validation analysis of the results and more in-depth

research will focus on some of the significantly changed proteins and pathways which we are interested in.

Conclusions

In the present study, rats were fed a high-fat diet and tandem mass tag-based proteomics techniques were used to study the effects of high-fat diet on rat liver. We identified a total of 198 significant differential proteins, and more new differentially expressed proteins were discovered. These significant differentially expressed proteins are primarily involved in lipid metabolism and glucose metabolism processes. In order to maintain physiological balance, the body inhibits fatty acid synthesis by regulating some key proteins, thereby promoting the oxidation of fatty acids and accelerating the degradation of fatty acids. These can be understood as the body's self-protection mechanism to counteract liver fat accumulation and degeneration. It is of great significance to study the mechanism of promoting the effect of high-fat diet on rat liver.

Acknowledgements

We are grateful to Shanghai Applied Protein Technology Co., Ltd for their technical assistance.

The study was supported by the Strategic Priority Research Program of the National Natural Science Foundation of China (no. 31571855 and no. 31701627).

J. S., R. G., Y. H., W. X. and C W. had substantial contributions to conception and design. H. Q., D. C., X. C., B. Y. and Y. H. had substantial contributions to data acquisition and analysis. J. S. and H. Q. drafted the article and revised it critically for important intellectual content. Y. H. and R. G. approved the final version to be published.

The authors declare that they have no conflicts of interest.

Supplementary material

For supplementary material/s referred to in this article, please visit https://doi.org/10.1017/S0007114519001740

References

1. Wardle J, Brodersen NH, Cole TJ, *et al.* (2006) Development of adiposity in adolescence: five year longitudinal study of an ethnically and socioeconomically diverse sample of young people in Britain. *BMJ* **332**, 1130–1135.
2. Cappel DA, Palmisano BT, Emfinger CH, *et al.* (2013) Cholesteryl ester transfer protein protects against insulin resistance in obese female mice. *Mol Metab* **2**, 457–467.
3. Visinoni S, Khalid NF, Joannides CN, *et al.* (2012) The role of liver fructose-1,6-bisphosphatase in regulating appetite and adiposity. *Diabetes* **61**, 1122–1132.
4. Vernon G, Baranova A, Younossi ZM, *et al.* (2011) Systematic review: the epidemiology and natural history of non-alcoholic fatty liver disease and non-alcoholic steatohepatitis in adults. *Aliment Pharmacol Ther* **34**, 274–285.
5. Mendes LL, Nogueira H, Padez C, *et al.* (2013) Individual and environmental factors associated for overweight in urban population of Brazil. *BMC Public Health* **13**, 988.
6. Halford JC, Boyland EJ, Blundell JE, *et al.* (2010) Pharmacological management of appetite expression in obesity. *Nat Rev Endocrinol* **6**, 255–269.
7. Woods SC, Seeley RJ, Rushing PA, *et al.* (2003) A controlled high-fat diet induces an obese syndrome in rats. *J Nutr* **133**, 1081–1087.
8. Benard O, Lim J, Apontes P, *et al.* (2016) Impact of high-fat diet on the proteome of mouse liver. *J Nutr Biochem* **31**, 10–19.
9. Houten SM, Denis S, Argmann CA, *et al.* (2012) Peroxisomal L-bifunctional enzyme (Ehhadh) is essential for the production of medium-chain dicarboxylic acids. *J Lipid Res* **53**, 1296–1303.
10. Fang X, Zhao Z, Jiang P, *et al.* (2017) Identification of the bovine HSL gene expression profiles and its association with fatty acid composition and fat deposition traits. *Meat Sci* **131**, 107–118.
11. Chevillard G, Clemencet MC, Etienne P, *et al.* (2004) Molecular cloning, gene structure and expression profile of two mouse peroxisomal 3-ketoacyl-CoA thiolase genes. *BMC Biochem* **5**, 3.
12. Poirier Y, Antonenkov VD, Glumoff T, *et al.* (2006) Peroxisomal β-oxidation—A metabolic pathway with multiple functions. *BBA-Mol Cell Res* **1763**, 1413–1426.
13. Van Veldhoven PP (2010) Biochemistry and genetics of inherited disorders of peroxisomal fatty acid metabolism. *J Lipid Res* **51**, 2863–2895.
14. Wanders RJ & Waterham HR (2006) Biochemistry of mammalian peroxisomes revisited. *Annu Rev Biochem* **75**, 295–332.
15. Davis MS, Solbiati J & Cronan JE, Jr. (2000) Overproduction of acetyl-CoA carboxylase activity increases the rate of fatty acid biosynthesis in *Escherichia coli*. *J Biol Chem* **275**, 28593–28598.
16. Kursula P, Ojala J, Lambeir AM, *et al.* (2002) The catalytic cycle of Biosynthetic thiolase: a conformational journey of an acetyl group through four binding modes and two oxyanion holes. *Biochemistry* **41**, 15543–15556.
17. Hundal RS, Krssak M, Dufour S, *et al.* (2000) Mechanism by which metformin reduces glucose production in type 2 diabetes. *Diabetes* **49**, 2063–2069.
18. Semple RK, Savage DB, Cochran EK, *et al.* (2011) Genetic syndromes of severe insulin resistance. *Endocr Rev* **32**, 498–514.
19. Wang X, Zhang Y, Zhang X, *et al.* (2017) The comprehensive liver transcriptome of two cattle breeds with different intramuscular fat content. *Biochem Biophys Res Commun* **490**, 1018–1025.
20. Tang SCW, Leung VTM, Chan LYY, *et al.* (2010) The acetyl-coenzyme A carboxylase beta (ACACB) gene is associated with nephropathy in Chinese patients with type 2 diabetes. *Nephrol Dial Transpl* **25**, 3931–3934.
21. Matsuoka H, Shima A, Kuramoto D, *et al.* (2015) Phosphoenolpyruvate carboxykinase, a key enzyme that controls blood glucose, is a target of retinoic acid receptor-related orphan receptor α. *PLOS ONE* **10**, e0137955.
22. Diazlobo M, Garciaamoros J, Fita I, *et al.* (2015) Correction: selective photoregulation of the activity of glycogen synthase and glycogen phosphorylase, two key enzymes in glycogen metabolism. *Org Biomol Chem* **13**, 10072–10072.
23. Bergman EN & Heitmann RN (1978) Metabolism of amino acids by the gut, liver, kidneys, and peripheral tissues. *Fed Proc* **37**, 1228–1232.
24. Cave MC, Clair HB, Hardesty JE, *et al.* (2016) Nuclear receptors and nonalcoholic fatty liver disease. *Biochim Biophys Acta* **1859**, 1083–1099.
25. Desvergne B & Wahli W (1999) Peroxisome proliferator-activated receptors: nuclear control of metabolism. *Endocr Rev* **20**, 649–688.
26. Mackenzie LS & Lione LJLS (2013) Harnessing the benefits of PPARβ/δ agonists. *Life Sci* **93**, 963–967.
27. Tanaka T, Yamamoto J, Iwasaki S, *et al.* (2003) Activation of peroxisome proliferator-activated receptor δ induces fatty acid

β-oxidation in skeletal muscle and attenuates metabolic syndrome. *Proc Natl Acad Sci U S A* **100**, 15924–15929.
28. Li JJ, Wang R, Lama R, *et al.* (2016) Ubiquitin ligase NEDD4 regulates PPARγ stability and adipocyte differentiation in 3T3-L1 Cells. *Sci Rep* **6**, 38550.
29. Cerda A, Hirata MH & Hirata RD (2014) Pharmacogenetics of drug metabolizing enzymes in Brazilian populations. *Drug Metabol Drug Interact* **29**, 153–177.
30. Sanwald P, David M & Dow J (1996) Characterization of the cytochrome P450 enzymes involved in the *in vitro* metabolism of dolasetron. Comparison with other indole-containing 5-HT3 antagonists. *Drug Metab Dispos* **24**, 602–609.
31. Fanni D, Ambu R, Gerosa C, *et al.* (2014) Cytochrome P450 genetic polymorphism in neonatal drug metabolism: role and practical consequences towards a new drug culture in neonatology. *Int J Immunopathol Pharmacol* **27**, 5–13.
32. Kostrubsky SE, Sinclair JF, Strom SC, *et al.* (2005) Phenobarbital and phenytoin increased acetaminophen hepatotoxicity due to inhibition of UDP-glucuronosyltransferases in cultured human hepatocytes. *Toxicol Sci* **87**, 146–155.
33. Debinski HS, Mackenzie PI, Lee CS, *et al.* (1996) UDP glucuronosyltransferase in the cirrhotic rat liver. *J Gastroenterol Hepatol* **11**, 373–379.

British Journal of Nutrition